Fibroblast activation protein regulates tumor-associated fibroblasts and epithelial ovarian cancer cells

DONGMEI LAI[1], LI MA[2] and FANGYUAN WANG[1]

[1]The International Peace Maternity and Child Health Hospital, School of Medicine, Shanghai Jiaotong University; [2]Zhangshan Hospital, Fudan University, Shanghai, P.R. China

Received January 20, 2012; Accepted March 26, 2012

DOI: 10.3892/ijo.2012.1475

Abstract. The fibroblast activation protein (FAP) is a cell surface serine protease which has emerged as a specific marker of tumor-associated fibroblasts (TAFs). FAP has been shown to have both *in vitro* dipeptidyl peptidase and collagenase activity. However, the biological function of FAP in the tumor microenvironment is largely unknown. In this study, we first show that TAFs isolated from ovarian cancer samples have the characteristics of stem cells. To explore the functional role of FAP, the protein was silenced by siRNA lentiviral vector transfection. FAP silencing inhibited the growth of TAFs *in vitro*, accompanied with cell cycle arrest at the G2 and S phase in TAFs. FAP silencing also reduced the stem cell marker gene expression in TAFs. SKOV3 cells do not express FAP. Although FAP-silenced SKOV3 cells induced ovarian tumors, the rate of tumor growth was significantly decreased, as shown in the xenograft mouse model. TAF phenotypes in the xenograft tumor tissues were further assayed by immunohistochemistry. The expression of TAF markers, including fibroblast-specific protein, FAP, smooth muscle actin, desmin, vascular endothelial growth factor and fibroblast growth factor was decreased in the tumor stroma induced by FAP-silenced SKOV3 cells. In conclusion, FAP is an important regulator of the microenvironment in tumor formation and targeting FAP is a potential therapeutic strategy to combat ovarian cancer.

Introduction

There is an increasing amount of experimental evidence that the tumor microenvironment [including fibroblastic stromal cells, infiltrating immune cells, blood and lymphatic vascular network and the extracellular matrix (ECM)] is an integral part of the carcinogenic process promoting cell growth and metastases (1-4). Fibroblastic stromal cells are also known as tumor-associated fibroblasts (TAFs), carcinoma-associated fibroblasts and reactive stroma. Most solid tumors, including ovarian cancer, have some degree of tumor stroma, with the finding of reactive stroma often being a poor prognostic indicator (5).

The fibroblast activation protein (FAP, also known as FAPα or seprase) has emerged as a specific marker of reactive fibroblasts in tumors. FAP is highly expressed in reactive stromal fibroblasts in more than 90% of human epithelial carcinomas, including breast, lung, colorectal and ovarian cancers (6). Neuronal and lymphoid cells, as well as the surrounding normal tissue, demonstrate a very weak FAP expression. Epithelial carcinoma cells are also FAP-negative. The function of FAP in the tumor microenvironment is largely unknown.

FAP is a type II transmembrane cell surface protein belonging to the serine protease family. *In vitro* studies have shown that FAP has both dipeptidyl peptidase and endopeptidase activity and is capable of degrading gelatin and type I collagen (7-10). The highly regulated expression and restricted distribution of FAP suggest that it could be a potential target for cancer therapy. A previous study demonstrated that the genetic deletion and pharmacological inhibition of FAP inhibited tumor growth in an endogenous lung cancer mouse model driven by the K-rasG12D mutant and in a colon cancer mouse model (11).

In this study, we demonstrate for the first time that primary ovarian TAFs have characteristic properties of stem cells. We then show that the transfection of FAP siRNA into SKOV3 cells inhibits the ovarian tumor growth *in vivo* and reduces tumorigenesis, although SKOV3 cells do not express FAP. Our results suggest that FAP is an important regulator of the microenvironment in tumor formation and its inhibition is a potential therapeutic approach for ovarian epithelial cancer treatment.

Materials and methods

Cell culture. Ovarian epithelial cancer specimens and normal ovarian samples were obtained with approval from the Institutional Review Boards at Shanghai Jiaotong University, Shanghai, China. The tumor samples were surgically removed from ovarian tumor sites whereas the controls were obtained from non-cancerous prophylactic oophorectomy specimens.

Correspondence to: Professor Dongmei Lai, The International Peace Maternity and Child Health Hospital, School of Medicine, Shanghai Jiaotong University, 910 Hengshan Road, Shanghai 200030, P.R. China
E-mail: laidongmei@hotmail.com

Key words: ovarian epithelial cancer, tumor-associated fibroblast, fibroblast activation protein, microenvironment

Tissue was washed, minced, suspended in McCoy's medium (Sigma-Aldrich, St. Louis, MO, USA) and mixed with 1% collagenase and 1% hyaluronidase (Invitrogen), followed by overnight incubation (37˚C, 5% CO_2). The enzymatically disaggregated cell suspensions were filtered (70-μm cell strainer) and washed twice with PBS. All the cells were separated on a gradient of Percoll Plus (the density of the top band and bottom layer was 45 and 90%, respectively) (GE Healthcare). The tumor cells were mostly found in the upper band and the TAFs were mainly found in the lower band. These two types of cells were separately maintained in two different culture systems. The tumor cells were cultured under standard conditions [DMEM/F12 supplemented with 10% fetal bovine serum (FBS)] and the attached cells showed a cobble-like morphology. The TAFs were maintained in DMEM containing 10% FBS and grown into elongated fibroblast-like cells. All cells were incubated at 37˚C in a humidified atmosphere containing 5% CO_2. The normal fibroblast cells (NFCs) were isolated in the same manner as described above.

Karyotype analysis. Chromosome analysis of the tumor cells and TAFs was performed using the G-band method.

RNA extraction and real-time qPCR analysis. Total RNAs were isolated from NFCs and TAFs using the RNeasy mini kit (Qiagen, Chataworth, CA, USA). Total RNA (500 ng) from each sample was used in reverse transcription (RT) using the iScript cDNA synthesis kit (Bio-Rad, Hercules, CA, USA). Real-time RT-qPCR was carried out on the cDNA using IQ SYBR-Green (Bio-Rad) on the Mastercycler ep realplex (Germany). All reactions were performed in a 25-ml volume. Primer sequences were listed in Table I. PCR was performed as previously reported (1,2).

Immunofluorescence staining. The TAFs and NFCs were fixed with 4% paraformaldehyde for 15 to 20 min at room temperature and then washed twice (10 min each) with 1X PBS. Cells were permeabilized with 0.1% Triton X-100 for 10 min at room temperature and then washed twice with 1X PBS. The cells were then blocked with blocking solution for 30 min and incubated with anti-Oct-4 (rabbit anti-human, 1:200; Chemicon, Temecula, CA, USA), anti-Nanog (rabbit anti-human, 1:200; Chemicon), anti-nestin (rabbit anti-human, 1:500; Santa Cruz Biotechnology, Santa Cruz, CA, USA), anti-FAP (rabbit anti-human, 1:500; Santa Cruz Biotechnology), anti-Vimentin (goat anti-human, 1:1,000; R&D Systems) and anti-human telomerase reverse transcriptase (hTERT) (rabbit anti-human, 1:1,000; Saierbio) antibodies for 1 h at room temperature. Cells were then washed three times with 1X PBS and probed with Cy3-labeled IgG (1:200; Jackson Immunoresearch, West Grover, PA, USA) antibody. Fluorescence images were captured using a Leica DMI3000 microscope.

Construction and production of FAP siRNA lentiviral vector. Lenti-shFAP-EGFP was constructed by inserting the shRNA sequence of FAP at the *Cla*/*Mlu*I site in the lentiviral vector, PLVTHM (FAP siRNA: sense, 5'-gacACGCGTCAGAAAGG TGCATATTACTTCAAGAGAGTAATATTGGCACCTTTC TTTTTTTCCAAATCGATgcc-3' and antisense, 3'-GGCA TCGATTTGGAAAAAAAGAAAGGTGCCAATATTACTC TCTTGAAGTAATATTGGCACCTTTCTGACGCGTGTC-5'; control siRNA, 5'-TGCGGAGGTGCCTATACCAC-3'). Lentiviral vectors were produced by transient transfection of 293T cells. Lentiviral vectors (20 μg), 10 μg pMDlg/pRRE, 5 μg pMD2.G and 5 μg pRSV-REV (a kind gift from Dr Trono) were mixed and brought to a volume of 250 μl with water. A total of 250 μl of 0.5 M $CaCl_2$ and 500 μl of HeBS2x (0.28 M NaCl, 0.05 M HEPES, 1.5 M Na_2HPO_4) was subsequently added and the mixture was allowed to sit on the bench for 30 min before transfection was performed. Dishes containing transfected cells were placed in a 37˚C humidified incubator with a 5% CO_2 atmosphere. The medium was aspirated 14 h later and 10 ml of fresh DMEM-10% FBS (PAA, Pasching, Austria) was gently added. After 28-h incubation, the virus was collected and cleared via centrifugation at 1,500 rpm for 15 min and filtration through a 0.45-μm filter. The sample was subsequently ultracentrifuged at 80,000 x g for 90 min. The supernatant was aliquoted and the pellet was resuspended with 1 ml PBS. Both the supernatant and the resuspended pellet were stored at -80˚C for future use. The titration of concentrated supernatants was performed by serial dilutions of vector stocks on $1x10^5$ HeLa cells followed by fluorescence-activated flow cytometry (Beckton-Dickinson Immunocytometry Systems). According to the formula: $1x10^5$ HeLa cell x % EGFP-positive cell x 1,000/μl virus, titers of lentiviral vectors were calculated among 0.1-$1x10^9$ TU/ml.

FAP silencing. TAFs (10^6) were grown to confluence in standard medium. For different applications, 5 μl FAP siRNA or control siRNA lentiviral vector were applied to the medium for 0-72 h.

Growth curve assay. The TAFs treated with FAP or control siRNA were plated in 48-well culture dishes with 500 μl of growth medium. Every two days 50 μl of medium were added to each well. The number of cells in each well was evaluated after 72 h of culture.

Cell cycle distribution analysis. The TAFs ($1x10^5$) treated with FAP siRNA or control siRNA for 48 h were suspended in hypotonic solution [0.1% Triton X-100, 1 mM Tris-HCl (pH 8.0), 3.4 mM sodium citrate, 0.1 mM EDTA] and then stained with 50 mg/ml of PI. The DNA content calculation was performed using a FC500 flow cytometer (Beckman Coulter) and analyzed by Beckman Coulter CXP software.

Western blot analyses. The TAFs ($1x10^5$) treated with FAP or control siRNA for 48 h were pooled and homogenized in the sample buffer. Total proteins were measured using the BCA kit (Pierce, Gaithersburg, MD, USA) according to the manufacturer's instructions. Protein (20 μg) was separated by SDS-PAGE and transferred to nitrocellulose membrane. Then the membrane was incubated with the primary antibody against FAP or β-actin (rabbit anti-human, 1:200; Boshide, Wuhan, China; or rabbit anti-human, 1:1,000; Cell Signaling Technology, Danvers, MA, USA) at room temperature overnight. This was followed by incubation with peroxidase-linked goat antirabbit-IgG (1:1,000, Santa Cruz Biotechnology) at room temperature for 1 h; then it was developed with a chemiluminescence reagent (Perkin-Elmer Life Sciences, Norwalk, CT, USA) and analyzed using the ChemiImager Imaging System (G:Box Syngene, Gene Company Ltd., Hong Kong, SAR, China).

Table I. PCR primer sequences.

Gene product	Forward (F) and reverse (R) primers (5'→3')	Size (bp)
Nanog	F: GGGCCTGAAGAAAACTATCCATCC R: TGCTATTCTTCGGCCAGTTGTTTT	400
Oct-4	F: GGCCCGAAAGAGAAAGCGAACC R: ACCCAGCAGCCTCAAAATCCTCTC	224
Sox2	F: GCGCGGGCGTGAACCAG R: CGGCGCCGGGGAGATACA	396
Nestin	F: CAGCTGGCGCACCTCAAGATG R: AGGGAAGTTGGGCTCAGGACTGG	208
CD133	F: TGGATGCAGAACTTGACAACGT R: ATACCTGCTACGACAGTCGTGGT	120
hTERT	F: GAGCTGACGTGGAAGATGAG R: CAGGATCTCCTCACGCAGAC	105
FAP	F: ATCTATGACCTTAGCAATGGAGAATTTGT R: GTTTTGATAGACATATGCTAATTTACTCCCAAC	163
18s RNA	F: CGTTGATTAAGTCCCTGCCCTT R: TCAAGTTCGACCGTCTTCTCAG	202

In vivo xenograft experiments. All animal studies adhered to the protocols approved by the Institutional Animal Care and Use Committee of Shanghai Jiao Tong University, Shanghai, China. The SKOV3 ovarian cancer cell line derived from high-grade serous adenocarcinoma was obtained from the Shanghai Cell Bank of the Chinese Academy of Sciences and maintained in McCoy's medium (Sigma-Aldrich) supplemented with 10% FBS. After the cells were grown to 80% confluence, 5 μl FAP or the control siRNA lentiviral vector were added to the medium. After 48 h, $1x10^8$ uninfected SKOV3 cells, control-transfected SKOV3 cells, or FAP siRNA transfected SKOV3 cells were separately injected subcutaneously (s.c.) into BALB/c mice (BALB/c-nu/nu, Harlan; each group n=5; total number, 15). Engrafted mice were inspected bi-weekly for tumor appearance by visual observation and palpation until a tumor was formed. Mice were sacrificed by cervical dislocation after 49 days. Xenograft tumors were removed, fixed in 10% phosphate-buffered formalin and embedded in paraffin for sectioning (5 mm) on a rotary microtome, followed by slide mounting for H&E staining and histological assessment or immunochemistry.

Immunohistochemical analysis. The sections were fixed for 5 min in neutral-buffered formalin, after which endogenous peroxidase activity was quenched by incubating the sections in 0.3% hydrogen peroxide in methanol for 30 min. The sections were treated with the following antibodies: rabbit anti-human fibroblast-specific protein (FSP), mouse anti-human FAP, mouse anti-human α-smooth muscle actin (α-SMA) (1:1,000 dilution; Biomeda, Foster City, CA), rabbit anti-human desmin (diluted 1:1,000; Novus Biologicals, Littleton, CO) and mouse anti-human vascular endothelial growth factor (VEGF), mouse anti-human epidermal growth factor (EGF) (1:1,000 dilution; Santa Cruz Biotechnology). For antibody detection, goat, rabbit or mouse peroxidase kits (Vector Laboratories, Burlingame, CA) were used following the manufacturer's instructions. Peroxidase substrate was developed by using the 3-amino-9-ethylcarbazole (AEC) and/or 3,39-diaminobenzidine (DAB) substrate kit (Vector Laboratories). The slides were counterstained with hematoxylin QS (Vector Laboratories) and were either mounted with low viscosity aqueous mounting medium (ScyTek Laboratories, Logan, UT) or dehydrated and mounted with VectaMount Permanent Mounting Medium (Vector Laboratories).

Statistics. Means, standard deviations, standard error and P-values (Student's t-tests) were calculated using Microsoft Excel. P-values <0.05 were considered to indicate statistically significant differences.

Results

Primary ovarian TAFs have distinct morphological phenotypes. The primary ovarian TAFs and primary epithelial ovarian cancer cells were harvested separately from the same ovarian cancer samples. When cultured under traditional conditions, the fibroblasts presented spindle-like morphologies and grew rapidly (Fig. 1A) whereas the ovarian epithelial cancer cells showed cobblestone-like characteristics and were relatively uniform epithelial cells (Fig. 1C). These two types of cells were morphologically distinguishable from each other. No karyotypic abnormality was found in the ovarian TAFs (Fig. 1B), suggesting that malignant changes had not occurred in these cells. On the contrary, the epithelial ovarian cancer cells displayed complex karyotypes, including multiple numerical and structural abnormalities of chromosomes (Fig. 1D).

Primary ovarian TAFs have characteristic properties of stem cells. The stem/progenitor cell phenotype has been found in ovarian cancer cells. We previously characterized a small population of ovarian cancer cells with stem cell properties, which

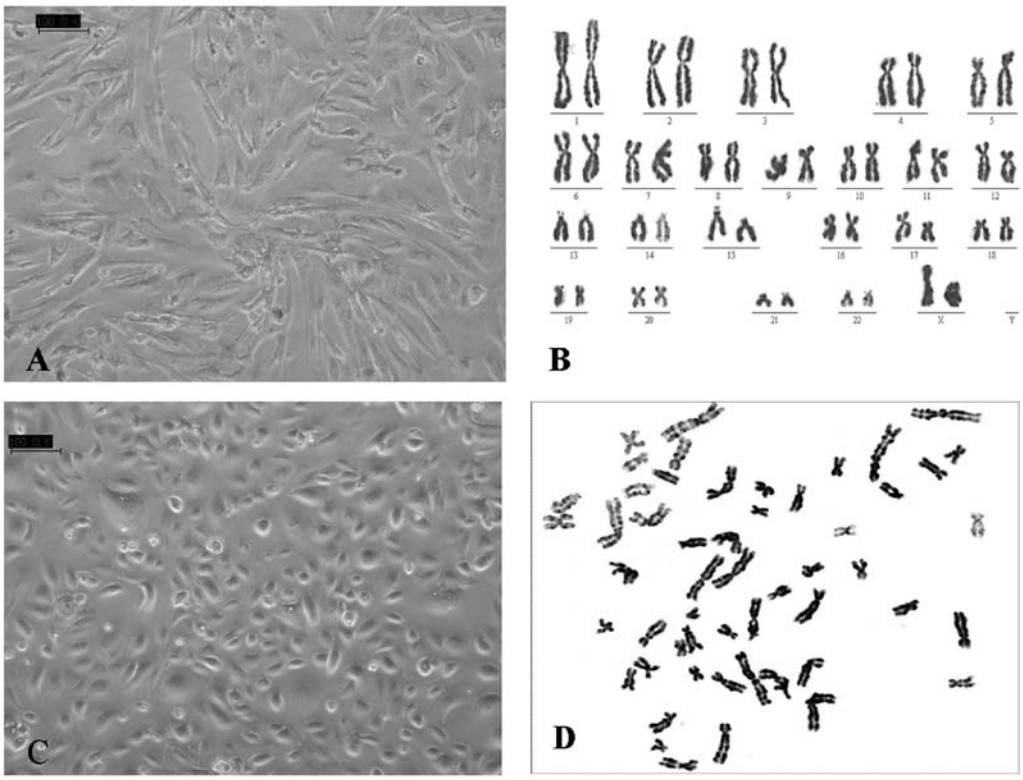

Figure 1. The fibroblasts and tumor cells were harvested separately from primary high-grade serous epithelial ovarian cancer. (A) The TAFs present spindle and spread morphologies. (B) The TAFs have the normal 46, XX chromosomes. (C) The ovarian cancer cells show cobblestone-like characteristics and are relatively uniform epithelial cells. (D) The ovarian cancer cells display chromosome abnormalities. Scale bars, 100 μm.

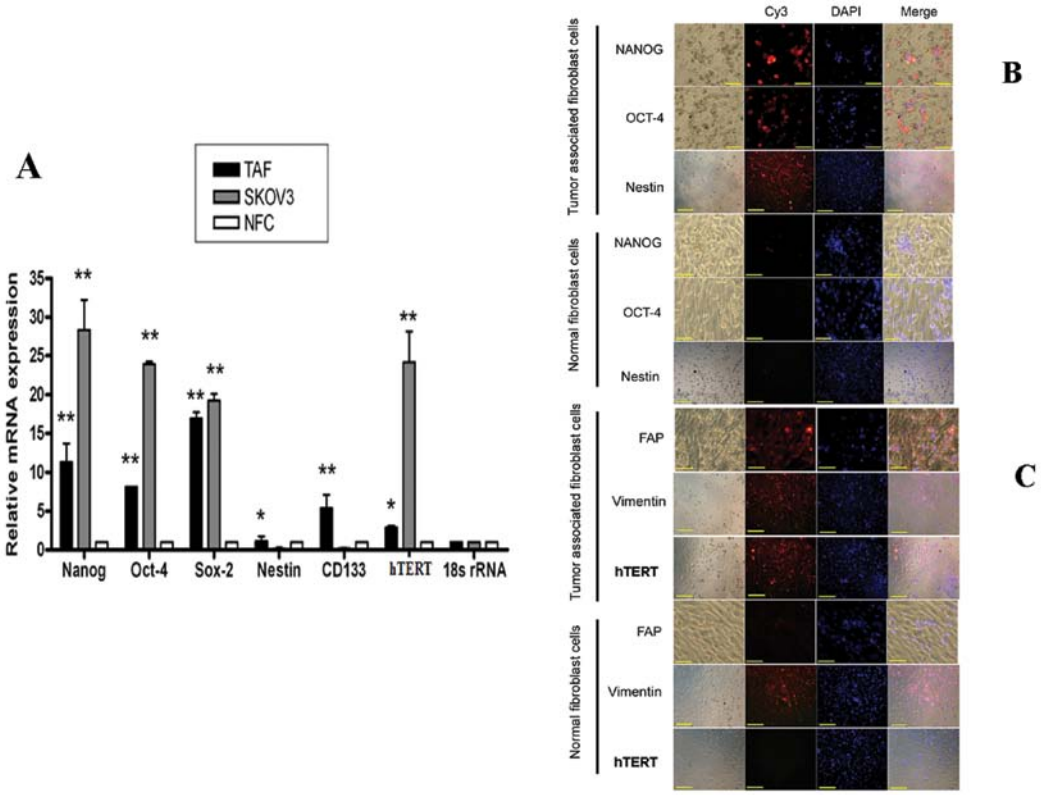

Figure 2. The primary ovarian TAFs have characteristic properties of stem cells. (A) As shown by real-time PCR, the expression of stem cell marker genes in TAFa was higher than that in NFCs, but lower than that in SKOV3 ovarian cancer cells (except for nestin and CD133). Values were calculated using 18s RNA as the internal control, *P<0.01, **P<0.001. (B) Representative double-staining for Oct-4, Nanog and nestin in TAFs and NFCs by immunofluorescence. (C) Immunofluorescence staining of anti-FAP, hTERT and Vimentin monoclonal antibodies in both TAFs and NFCs (Cy3-labeled secondary antibody, red; nucleus immunofluorescence stained with DAPI, blue; merged image between Cy3 and DAPI). Scale bars, 100 μm.

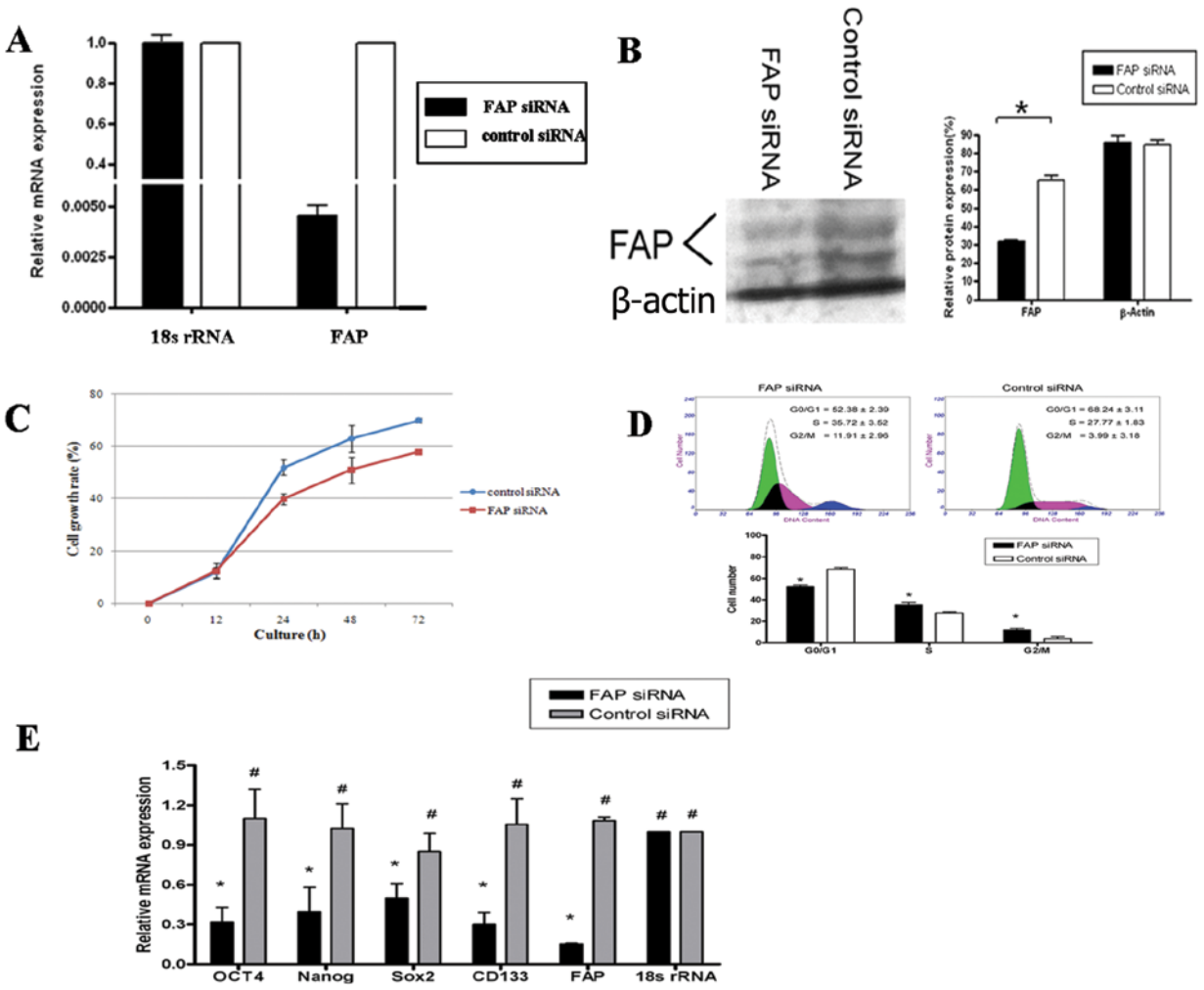

Figure 3. FAP siRNA inhibits the growth of TAF cells *in vitro*. FAP siRNA inhibited FAP expression in TAFs to approximately 50% of the controls as indicated by (A) quantitative RT-PCR and (B) western blot analysis. (C) Compared with the control siRNA-infected TAFs, FAP siRNA affected the cell growth of TAFs and (D) increased the population of cells at the G2 and S phase, with a reduction of cells at the G1 phase. (E) FAP siRNA inhibited the stem cell gene expression in TAFs compared with mock transfection. *P<0.01, #P>0.05.

is believed to be responsible for tumor initiation, progression, metastasis and drug resistance (12,13). The TAFs have distinct morphological phenotypes that differ from normal fibroblasts; however, the phenotypic and functional heterogeneity among TAFs is yet to be fully explored. In this study, we examined the expression of putative stem cell markers in TAFs. Quantitive real-time PCR showed that the expression of Nanog, Oct-4, Sox2, nestin, CD133 and hTERT in TAFs was higher than that in NFCs, but lower than that in ovarian cancer cells (except for nestin and CD133, Fig. 2A) (P<0.01). The expression of the transcription factors, Oct-4, Nanog and nestin, was further investigated by immunostaining and it was found that TAFs had staining patterns for these genes compared with the NFCs (Fig. 2B). Both the normal fibroblasts and TAFs had staining for Vimentin, which is the most frequently found intermediate filament in fibroblasts. Thus, it is a reliable fibroblast marker. FAP has emerged as a marker of TAFs and FAP is expressed only by TAFs and not by NFCs (Fig. 2C). Of note, TAFs also showed increased expression of hTERT compared with NFCs (Fig. 2C).

FAP siRNA inhibits the growth of TAFs in vitro. Experimental evidence suggests that in primary tumors, FAP is expressed only by TAFs and pericytes but not by tumor cells. However, the mechanisms involved have not been defined. In this study, to determine whether FAP promotes tumorigenesis and to understand the molecular mechanism by which this might occur under more relevant pathophysiological conditions, we examined the impact of FAP siRNA on TAFs. We constructed the lentiviral vector encoding FAP siRNA and silenced TAFs with FAP siRNA. This reduced FAP expression in TAFs to approximately 50% of the control level (determined by quantitative RT-PCR and western blot analysis) (Fig. 3A and B). In addition, after transfection with FAP siRNA, the silenced TAFs grew at a slower rate than the control cells as revealed by the MTT assay (P<0.05, Fig. 3C).

The effects of FAP siRNA on the TAF cell cycle progression were further investigated. The TAFs infected with FAP or control siRNA were analyzed for cell cycle distribution by means of flow cytometry. Compared with the control siRNA-infected TAFs, cells transfected with FAP siRNA had an increased population at the G2 and S phase and a reduced number in the G1 phase (P<0.01, Fig. 3D). These results indicated that FAP silencing led to cell cycle arrest at the G2 and S phase in TAFs. Of note, the FAP siRNA also significantly inhibited the stem

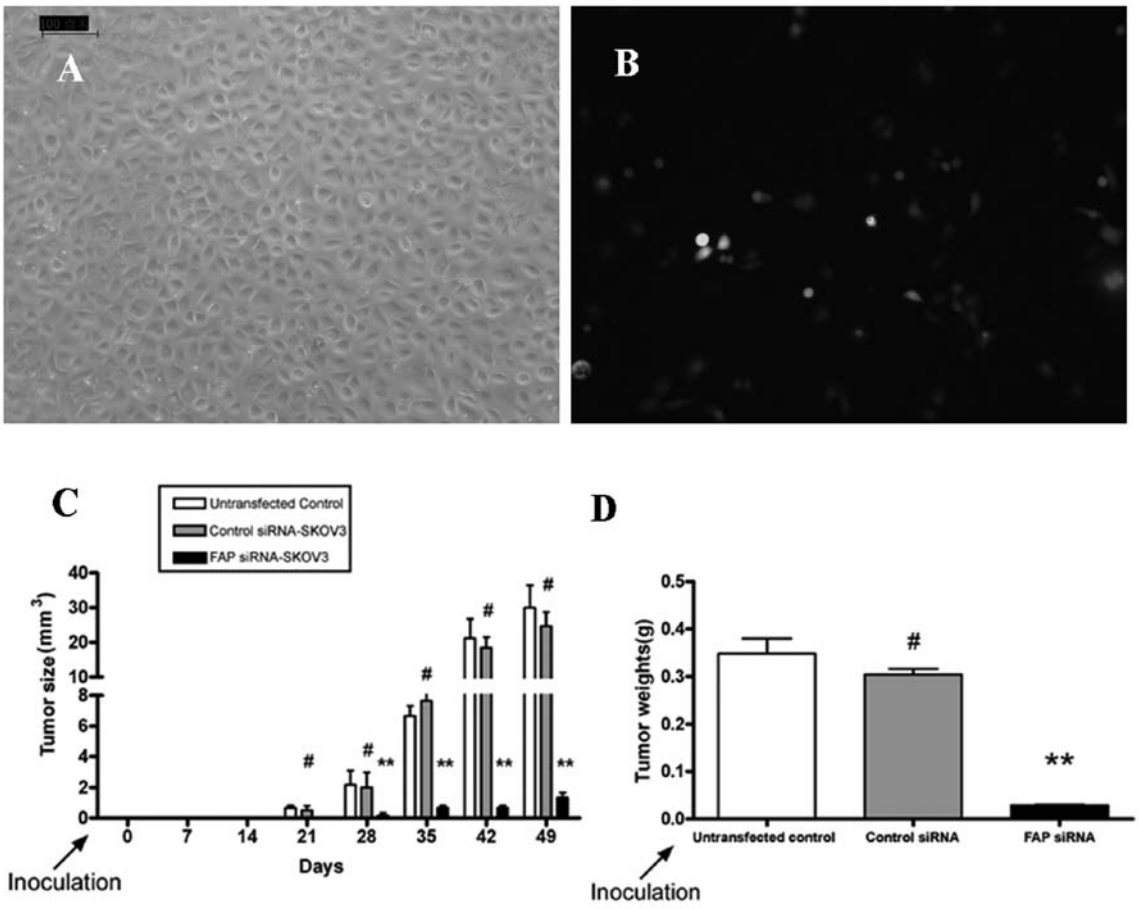

Figure 4. FAP siRNA inhibits the ovarian tumor development in nude mice. (A) SKOV3 ovarian cancer cells were cultured to 80% confluence. (B) Ovarian cancer cells transfected with FAP siRNA encoding green fluorescence protein (GFP). After 24 h, these cells expressed GFP. (C) Uninfected, mork-transfected, or FAP siRNA-transfected SKOV3 cells ($1x10^7$) were separately injected s.c. into Balb/c mice. Tumor size and weight were measured in the three groups (five to six per group in each of three independent experiments). The sizes of xenograft tumord induced by FAP siRNA-transfected SKOV3 cells were significantly smaller than those of tumors induced by mork-transfected or untransfected SKOV3 cells. ($^{**}P<0.001$). (D) Tumor weight was significantly different between the FAP siRNA-transfected group and the controls ($^{**}P<0.001$). There was no difference in tumor size and weight between the untransfected and mock-transfected groups ($^{\#}P>0.05$).

cell gene expression in TAFs. Quantitive real-time PCR showed that the expression of Nanog, Oct-4, Sox2 and CD133 in the FAP siRNA-transfected TAFs was lower than that in the control siRNA-transfecteds TAF (Fig. 3E).

FAP siRNA inhibits ovarian tumor growth in vivo and reduces tumorigenesis. Uninfected, mock-infected, or FAP siRNA-infected SKOV3 cells were separately injected s.c. into BALB/c mice. All three groups developed tumors, but the FAP siRNA-infected SKOV3 cells reduced the tumor burden in mice. Overall, the tumor volume and weight in the FAP siRNA-transfected group were significantly reduced compared with those in the mock control and untransfected groups (Fig. 4C and D).

H&E micrographs showed that ovarian cancer samples from the mock-transfected SKOV3 cells in nude mice had much more stromal cells in the tumor tissues, whereas the ovarian cancer samples from the FAP siRNA-transfected SKOV3 cells had less stromal cells (Fig. 5A and B). To quantify cell proliferation in each group, Ki67 immunohistochemistry (IHC) assay was performed in the representative tumor regions. Ki67-positive cells were markedly different in both groups and the proliferative index in the control was much higher than that in the FAP siRNA-silenced tumors (Fig. 5C-E). These results indicated that the reduced tumor growth was associated with a reduction in the proliferative index of tumors based on Ki67 staining.

FAP activity regulates tumor stromagenesis and angiogenesis. H&E staining showed that the control tumors had a larger stromal area compared to the FAP siRNA-treated tumors (Fig. 5A and B). IHC of FAP and FSP expression was further conducted on the tumor sections to identify TAF characteristics. FSP and FAP staining was evident within the stromal area in the uninfected SKOV3 or mock-infected SKOV3 tumors but not in the FAP siRNA-treated tumors (Fig. 6A and B).

The other characteristic of TAFs is the expression of myofibroblastic markers, including α-SMA, desmin and another marker of neo-microvascularization, VEGF. In the control tumors, IHC staining revealed an expression pattern of both α-SMA and desmin (Fig. 6D and E). VEGF expression was strong in the stromal cells, but was not distributed in the tumor cells. These patterns of expression were not evident in the FAP siRNA SKOV3 tumors (Fig. 6F). The α-SMA staining is an indicator of microvascularization within the tumor and is

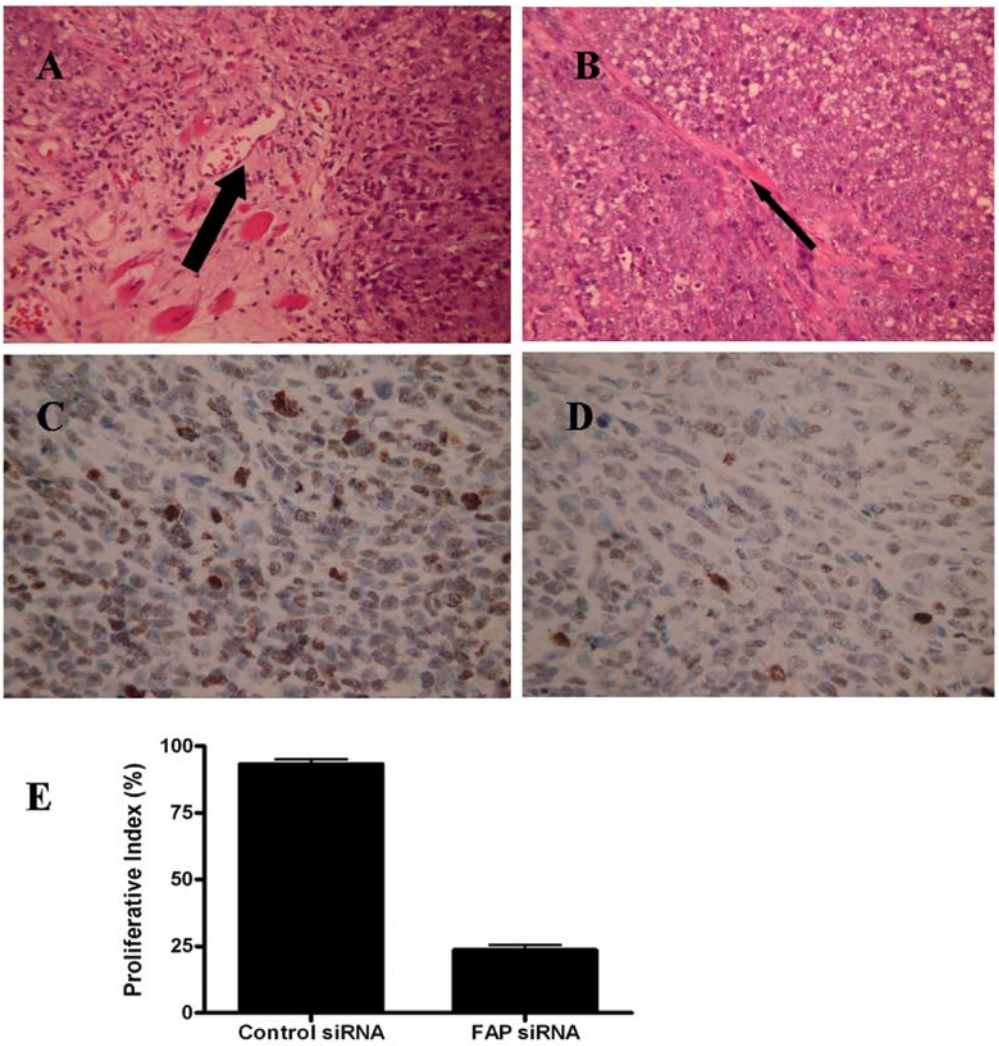

Figure 5. FAP siRNA attenuates tumor cell proliferation and alters tumor morphology. (A) Representative H&E micrographs of sections of ovarian cancer from mock-transfected SKOV3 cells in nude mice, which had much more stromal cells (arrows) in the tumor tissues. (B) H&E staining of sections of ovarian cancer from FAP siRNA-transfected SKOV3 cells in nude mice, which had less stromal cells (arrows) in the tumor tissues. (C and D) Ki67 immunohistochemistry in representative tumor regions in the control and FAP-siRNA-transfected tumors, respectively. (E) The different proliferative index of tumors grown in the two groups of mice ($P<0.0001$). Original magnification, x100.

a contributing factor to the TAF phenotype within the tumor microenvironment. In the control tumors, we found that SMA was overexpressed in the fibroblast cells around the tumor cells, while the tumor cells were not positive for SMA staining.

The expression of the growth factor, EGF, in TAFs was also detected in the tumors. The growth factors produced by TAF may support tumor development and metatasis. We found that EGF staining by IHC was present at concentrated amounts on the leading edge of the tumors where a large portion of stroma is found in the control vector-infected SKOV3 tumors as compared to the FAP siRNA-infected SKOV3 tumors (Fig. 6C). Growth factor staining was also found in the membrane of tumor cells due to the fact that tumor cells also secrete the growth factor, EGF.

Discussion

Tumors are composed of heterogeneous populations of cells, including transformed cells and a multitude of untransformed cells, including inflammatory and immune cells, endothelial cells and TAFs. TAFs have been shown to promote tumor growth by inducing angiogenesis and remodeling the ECM. TAFs also mediate epithelial mesenchymal transition (EMT) in tumor cells (14). A subset of TAFs are phenotypically and functionally distinguishable from normal fibroblasts, but are characterized as reactive fibroblasts in tumors, based on the expression of FAP.

Although a considerable number of studies have suggested that FAP expression in the tumor microenvironment promotes tumor growth and metastasis (15,16), its potential role has yet to be fully investigated. This study provides the first direct demonstration that the silencing of FAP inhibits the growth of TAFs and decreases their stemness. Furthermore, targeting FAP in SKOV3 tumor cells results in tumor growth inhibition.

A number of studies have revealed that the highly tumorigenic cancer progenitor cells expressing stem cell-like markers, such as CD133, CD44, Oct-3/4, c-KIT and/or xenobiotic efflux pumps associated with multidrug resistance, have been isolated from ovarian cancers and tumors established with cancer cell

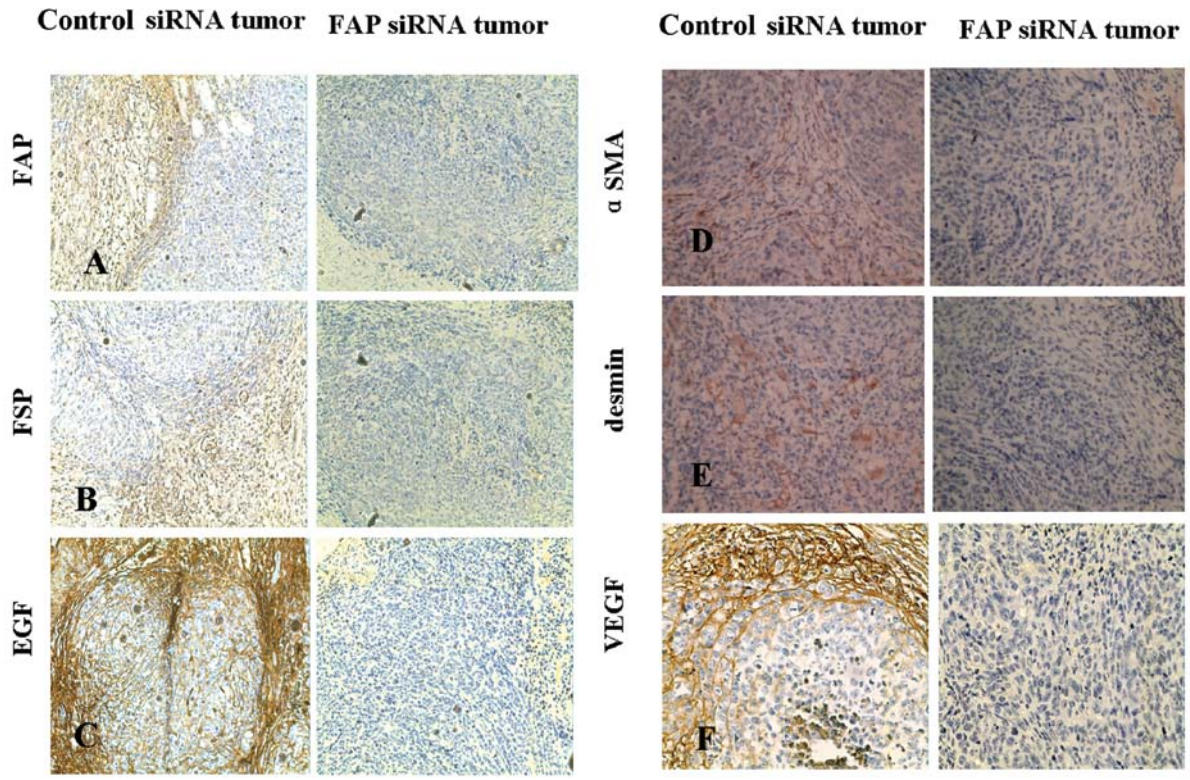

Figure 6. FAP siRNA inhibits the expression of fibroblast markers and provascularization markers indicative of TAFs within the tumor microenvironment in SKOV3 xenografts. IHC staining for markers that define fibroblast presence are visible in the control siRNA-transfected SKOV3 tumors but not in the FAP siRNA-silenced SKOV3 xenografts. (A) The fibroblast markers, FAP and (B) FSP, are both present throughout the control tumors. Likewise, (C) EGF is highly expressed in the stromal regions of the control SKOV3 tumors. One characteristic of TAFs is their ability to form fibrovascular networks, which include vessels and the architectural foundation in which they lay. (D) IHC staining reveals structural proteins α-SMA and (E) desmin as well as factors suggestive of tumor vascularization, including (F) VEGF in the control tumors but not in the FAP siRNA-silenced tumors. Original magnification, x200.

lines (17-19). These cancer progenitor cells have also been designated as cancer stem cells or cancer-initiating cells, which are able to give rise to more differentiated cancer cell types *in vitro* and *in vivo* and appear to play a critical role in tumor formation, progression and metastasis. To further demonstrate the characteristics of TAFs and NFCs, we examined their stem cell gene expression. We found that the expression of stem cell genes was higher in TAFs than that in normal fibroblasts. A number of studies have demonstrated that normal fibroblasts play a role in maintaining epithelial homeostasis by suppressing the proliferation and oncogenic potential of adjacent epithelia (20,21). The cellular origin of TAFs remains unclear; however, following the neoplastic transformation of epithelia, some TAFs are recruited to the expanding tumor mass from local tissue fibroblasts (15) and additional TAFs can be recruited from peripheral fibroblast pools, such as bone marrow-derived mesenchymal stem cells (MSCs) (22). Spaeth *et al* provided evidence that TAFs are derived from MSCs that acquire a TAF phenotype following exposure to or systemic recruitment into a xenograft ovarian adenocarcinoma model (23). In this manner, the upregulated expression of diverse tumorigenic target gene products in cancer progenitor cells and their progeny induced through the activation of distinct developmental signaling pathways, such as EGF/epidermal growth factor receptor (EGFR), hedgehog, Wnt/β-catenin, Notch, tumor growth factor-β (TGF-β) and/or integrin cascades may co-operatively participate in the formation of TAFs (24). Thus, the acquisition of stem cell characteristics of the fibroblasts may be determined by their source. Recently published data suggest that TAF-induced EMT leads to the enhanced expression of stem cell markers in prostate carcinoma cells, and increases the ability of these cells to form prostaspheres and to self-renew (25). Thus, the paracrine interplay between TAFs and cancer cells leads to the maintaining of cancer stem cell properties associated with aggressiveness and metastatic spread.

In this study, we found that TAFs with overexpressed hTERT, the catalytic subunit of telomerase, have normal karyotypes. Telomerase overexpression has already been associated with carcinogenesis. A previous study described the karyotypic stability of human fibroblasts immortalized by the expression of hTERT. The ectopic overexpression of telomerase is associated with unusual spontaneous as well as radiation-induced chromosome instability (26). These results confirm that TAFs maintain their genome stability by a telomere-independent mechanism and are possibly more genetically stable than tumor cells.

The expression of human FAP is highly specific for tumor fibroblasts. FAP is heavily expressed in reactive stromal fibroblasts in >90% of human epithelial carcinomas including breast, lung, colorectal and ovarian. Neuronal and lymphoid cells, as well as the surrounding normal tissue, demonstrate a very weak FAP expression (6). Cheng *et al* reported that HEK293 cells ectopically overexpressing FAP, when xenografted into scid mice, were 2-4-fold more likely to develop tumors and showed that FAP increased tumorigenicity and significantly enhanced tumor growth (27). They also found that enzymatic

mutants of FAP that are devoid of FAP enzymatic activity, when xenografted into immunodeficient mice, resulted in attenuated tumor growth (28). In the present study, we found that silencing FAP inhibited the growth of TAFs, accompanied with cell cycle arrest at the G2 and S phase. Of note, FAP siRNA transfection also significantly inhibited the stem cell gene expression in TAFs.

Epithelial carcinoma cells are FAP-negative. Consistently, we found that FAP was not expressed in SKOV3 cells (data not shown). Recently, Mentlein *et al* reported that FAP was detected at low levels in gliospheres (glioma stem-like cells); however, when these cells were induced to differentiate in 10% fetal calf serum, FAP expression was considerably increased (29). To date, little is known about the presence of FAP in tumor cells. We found that FAP siRNA-infected SKOV3 cells induced tumors in mice. However, FAP silencing significantly reduced both the tumor volume and tumor weight compared with the mock control and uninfected SKOV3 cells. Importantly, the reduced tumor growth was associated with a reduction in the proliferative index of tumors based on staining with Ki67. These results provide evidence showing the importance of FAP in tumorigeness regulation.

The TAF population differs from a normal fibroblastic phenotype and is defined as an activated fibroblast population, which is a rich source of tumor growth-promoting and pro-angiogenic factors. TAFs have distinct myofibroblastic characteristics. Qualifying factors that characterize TAFs include: i) the fibroblast markers, FSP and FAP; ii) myofibroblast/provascularizing potential including desmin, α-SMA and VEGF; and iii) growth factors, such as TGF-β, basic fibroblast growth factor (bFGF) and EGF (30). In the current study, through IHC, we observed the role of FAP in the formation of fibrovascular structure and 'TAF characteristics' by FAP silencing within established xenograft tumor models. We identified the neovascular, fibroblastic and matrix remodeling nature of TAFs in the tumor microenvironment. The two markers, FAP and FSP, which were overexpressed in TAFs as compared to normal fibroblasts, were evident in SKOV3 tumor sections treated with control vector, but not evident in the SKOV3 tumor sections treated with FAP siRNA by IHC staining (Fig. 6A and B). The other characteristic was the expression of typical myofibroblast-associated proteins. Desmin is a muscle-specific, intermediate filament protein common in myofibrils (31). The expression pattern of desmin was different from that of α-SMA in SKOV3 tumors treated with the control vector (Fig. 6D and E). However, the expression of both desmin and α-SMA was decreased in the stromal regions of the SKOV3 tumors treated with FAP siRNA silencing. Our data suggest that FAP contributes to the neovascularization within SKOV3 tumors. The final characteristic that defines TAFs is the expression of tumor-supportive growth factors, including VEGF and EGF. TAFs biologically impact tumor progression through the production of growth factors, cytokines, chemokines, matrix-degrading enzymes and immunomodulatory mechanisms. In our *in vivo* studies, VEGF and EGF were highly expressed in the stromal compartments of the SKOV3 tumors treated with the control vectors, but poorly expressed in the tumors treated with FAP siRNA silencing. The presence of FAP may have an impact on growth factor production in TAFs. Kraman *et al* created FAP knock-out transgenic mouse and found that the depletion of FAP-expressing cells made up only 2% of all tumor cells in established Lewis lung carcinomas, caused rapid hypoxic necrosis of both cancer and stromal cells in immunogenic tumors involving interferon-γ and tumor necrosis factor-α (Kraman *et al*). Thus, the TAF population is an immune-suppressive component of the tumor microenvironment (32).

In conclusion, we show that TAFs have the characteristics of stem cells and that FAP silencing in TAFs inhibits cell growth *in vitro* as well as stem cell gene expression. In addition, we show that FAP silencing in SKOV3 cells induces ovarian tumors, but significantly reduces tumor growth in the xenograft mouse model, accompanied with the decrease of TAF characteristics. Clearly, FAP plays an important role in the tumorigeness, stromagenesis and angiogenesis of ovarian cancer and targeting FAP is a potential therapeutic strategy for ovarian cancer patients.

Acknowledgements

This study was supported by grants from the Shanghai Municipal Council for Science and Technology (no. 09411968300), the Key Project Fund of Shanghai Municipal Health Bureau (2010011) and by the National Natural Science Foundation of China (NSFC; project no. 81070533).

References

1. Kunz-Schughart LA and Knuechel R: Tumor-associated fibroblasts (part I): active stromal participants in tumor development and progression? Histol Histopathol 17: 599-621, 2002.
2. Kunz-Schughart LA and Knuechel R: Tumor-associated fibroblasts (part II): functional impact on tumor tissue. Histol Histopathol 17: 623-637, 2002.
3. Orimo A, Gupta PB, Sgroi DC, *et al*: Stromal fibroblasts present in invasive human breast carcinomas promote tumor growth and angiogenesis through elevated SDF-1/CXCL12 secretion. Cell 121: 335-348, 2005.
4. Rowley DR: What might a stromal response mean to prostate cancer progression? Cancer Metastasis Rev 17: 411-419, 1998.
5. Ostermann E, Garin-Chesa P, Heider KH, *et al*: Effective immunoconjugate therapy in cancer models targeting a serine protease of tumor fibroblasts. Clin Cancer Res 14: 4584-4592, 2008.
6. Garin-Chesa P, Old LJ and Rettig WJ: Cell surface glycoprotein of reactive stromal fibroblasts as a potential antibody target in human epithelial cancers. Proc Natl Acad Sci USA 87: 7235-7239, 1990.
7. Christiansen V, Jackson KW, Lee KN and McKee PA: Effect of fibroblast activation protein and alpha2-antiplasmin cleaving enzyme on collagen types I, III, and IV. Arch Biochem Biophys 457: 177-186, 2007.
8. Aggarwal S, Brennen WN, Kole TP, *et al*: Fibroblast activation protein peptide substrates identified from human collagen I derived gelatin cleavage sites. Biochemistry 47: 1076-1086, 2008.
9. Piñeiro-Sánchez ML, Goldstein LA, Dodt J, *et al*: Identification of the 170-kDa melanoma membrane-bound gelatinase (seprase) as a serine integral membrane protease. J Biol Chem 272: 7595-7601, 1997.
10. Park JE, Lenter MC, Zimmermann RN, *et al*: Fibroblast activation protein, a dual specificity serine protease expressed in reactive human tumor stromal fibroblasts. J Biol Chem 274: 36505-36512, 1999.
11. Santos AM, Jung J, Aziz N, Kissil JL and Puré E: Targeting fibroblast activation protein inhibits tumor stromagenesis and growth in mice. J Clin Invest 119: 3613-3625, 2009.
12. Liu T, Cheng WW, Lai DM, Huang Y and Guo LH: Characterization of primary ovarian cancer cells in different culture systems. Oncol Rep 23: 1277-1284, 2010.
13. Ma L, Lai DM, Liu T, Cheng WW and Guo LH: Cancer stem-like cells can be isolated with drug selection in human ovarian cancer cell line SKOV3. Acta Biochim Biophys Sin 42: 593-602, 2010.

14. Giannoni E, Bianchini F, Calorini L and Chiarugi P: Associated fibroblasts exploit reactive oxygen species through a proinflammatory signature leading to epithelial mesenchymal transition and stemness. Antioxid Redox Signal 14: 2361-2371, 2011.
15. Studeny M, Marini FC, Champlin RE, *et al*: Bone marrow-derived mesenchymal stem cells as vehicles for interferon-beta delivery into tumors. Cancer Res 62: 3603-3608, 2002.
16. Nakamizo A, Marini F, Amano T, *et al*: Human bone marrow-derived mesenchymal stem cells in the treatment of gliomas. Cancer Res 65: 3307-3318, 2005.
17. Al-Hajj M and Clarke MF: Self-renewal and solid tumor stem cells. Oncogene 23: 7274-7282, 2004.
18. Fang D, Nguyen TK, Leishear K, *et al*: A tumorigenic subpopulation with stem cell properties in melanomas. Cancer Res 65: 9328-9237, 2005.
19. Bapat SA, Mali AM, Koppikar CB and Kurrey NK: Stem and progenitor-like cells contribute to the aggressive behavior of human epithelial ovarian cancer. Cancer Res 65: 3025-3029, 2005.
20. Baglole CJ, Maggirwar SB, Gasiewicz TA, *et al*: The aryl hydrocarbon receptor attenuates tobacco smoke-induced cyclooxygenase-2 and prostaglandin production in lung fibroblasts through regulation of the NF-kappaB family member RelB. J Biol Chem 283: 28944-28957, 2008.
21. Trimboli AJ, Cantemir-Stone CZ, Li F, *et al*: Pten in stromal fibroblasts suppresses mammary epithelial tumours. Nature 461: 1084-1091, 2009.
22. Studeny M, Marini FC, Dembinski JL, *et al*: Mesenchymal stem cells: potential precursors for tumor stroma and targeted-delivery vehicles for anticancer agents. J Natl Cancer Inst 96: 1593-1603, 2004.
23. Spaeth EL, Dembinski JL, Sasser AK, *et al*: Mesenchymal stem cell transition to tumor-associated fibroblasts contributes to fibrovascular network expansion and tumor progression. PLoS One 4: e4992, 2009.
24. Mimeault M and Batra SK: Interplay of distinct growth factors during epithelial mesenchymal transition of cancer progenitor cells and molecular targeting as novel cancer therapies. Ann Oncol 18: 1605-1619, 2007.
25. Giannoni E, Bianchini F, Masieri L, *et al*: Reciprocal activation of prostate cancer cells and cancer-associated fibroblasts stimulates epithelial-mesenchymal transition and cancer stemness. Cancer Res 70: 6945-6956, 2010.
26. Pirzio LM, Freulet-Marrière MA, Bai Y, *et al*: Human fibroblasts expressing hTERT show remarkable karyotype stability even after exposure to ionizing radiation. Cytogenet Genome Res 104: 87-94, 2004.
27. Cheng JD, Dunbrack RL Jr, Valianou M, *et al*: Promotion of tumor growth by murine fibroblast activation protein, a serine protease, in an animal model. Cancer Res 62: 4767-4772, 2002.
28. Cheng JD, Valianou M, Canutescu AA, *et al*: Abrogation of fibroblast activation protein enzymatic activity attenuates tumor growth. Mol Cancer Ther 4: 351-360, 2005.
29. Mentlein R, Hattermann K, Hemion C, Jungbluth AA and Held-Feindt J: Expression and role of the cell surface protease seprase/fibroblast activation protein-α (FAP-α) in astroglial tumors. Biol Chem 392: 199-207, 2011.
30. Littlepage LE, Egeblad M and Werb Z: Coevolution of cancer and stromal cellular responses. Cancer Cell 7: 499-500, 2005.
31. Lazarides E, Granger BL, Gard DL, *et al*: Desmin- and vimentin-containing filaments and their role in the assembly of the Z disk in muscle cells. Cold Spring Harbor Symp Quant Biol 46: 351-378, 1982.
32. Kraman M, Bambrough PJ, Arnold JN, *et al*: Suppression of antitumor immunity by stromal cells expressing fibroblast activation protein-alpha. Science 330: 827-830, 2010.